Prescribed Performance Backstepping Control of Flexible Joint Based on Unknown State Estimator and Improved Tracking Differentiator

SONG Chuanming, DU Qinjun, PANG Hao, LI Cunhe, JIAO Ticao*

School of Electrical and Electronic Engineering, Shandong University of Technology, Zibo 255049, P. R. China

(Received 10 August 2022; revised 6 December 2022; accepted 20 February 2023)

Abstract: In order to solve the problem of increasing tracking error of flexible joint system caused by model uncertainty and external unknown disturbance, a prescribed performance backstepping control method based on unknown state estimator and tracking differentiator is proposed. An unknown state estimator based on low-pass filter is designed, which can estimate the lumped disturbance only depending on the nominal value of the model. A novel finite-time convergence prescribed performance function is constructed. Based on this function, a backstepping controller is designed to ensure that all signals in the closed-loop system are bounded, and the joint tracking error converges to any given small area within the given time. To avoid the differential explosion of the backstepping controller, a tracking differentiator based on the improved Sigmoid function is designed to estimate the differential signal of virtual control law. The simulation results show that the proposed method can guarantee the joint tracking error converges to any given range within the finite time under the disturbance of unmodeled dynamics and unknown input, and can effectively improve the transient and steady-state performance of flexible joints.

Key words: flexible joint; unknown state estimator; tracking differentiator; prescribed performance control; backstepping control

CLC number: TP273 **Document code:** A **Article ID:** 1005-1120(2023)03-0336-18

0 Introduction

Robots with flexible joints are widely used in various scenes[1-2], which require higher control accuracy of flexible joints. The model-based control method is considered to be one of the most effective methods. However, it is difficult to establish an accurate dynamic model of the flexible joint system. Factors such as joint hardware parameter errors, nonlinear modes, and joint stiffness changes will cause a large deviation between the theoretical model and the actual system, thereby reducing the model-based control accuracy. In addition, flexible joints usually need to face various unknown external disturbances in complex environments. These unknown disturbances will increase the joint tracking error and even cause the system to lose control[3-4]. Therefore, improving the tracking accuracy of flexible joints under the influence of unknown disturbances is the focus of research.

In general, the unknown disturbances of flexible joint system mainly come from unmodeled dynamics and external disturbances. In order to reduce the joint tracking error, Davis et al.[5] proposed a computational torque control method, but this method relies on an accurate dynamic model, which is almost impossible in practical application. Robust control and adaptive control are considered effective control methods for dealing with unknown disturbances[6-7]. However, there is no unified parameter tuning method for adaptive control, which increases the difficulty of its application. The neural network

*Corresponding author, E-mail address: duqinjun@sdut.edu.cn.

How to cite this article: SONG Chuanming, DU Qinjun, PANG Hao, et al. Prescribed performance backstepping control of flexible joint based on unknown state estimator and improved tracking differentiator[J]. Transactions of Nanjing University of Aeronautics and Astronautics, 2023, 40(3): 336-353.

http://dx.doi.org/10.16356/j.1005-1120.2023.03.009

has a strong nonlinear fitting ability, and it can better approximate and compensate the unmodeled dynamics of the system[8-9]. However, the large amount of calculation and slow convergence speed of the neural network will reduce the transient performance of the system. In recent years, the development of observers has provided effective tools for estimating unmodeled dynamics and external disturbances. For example, Xi et al.[10] designed a sliding mode disturbance observer (SMDOB). Xue et al.[11] proposed an extended state observer (ESO) for estimating uncertain nonlinear disturbances. Xu et al.[12] proposed an unscented Kalman filter (UKF). These studies provide new methods and ideas for the uncertainty estimation of robot systems, but the design of these observers usually needs to calculate the inverse of the coefficient matrix and depends on the accurate system dynamics model. Na et al.[13] proposed a design method for unknown state estimator, which is simple in structure and easy to tune parameters, but it still needs further improvement in reducing model dependence.

The above research is devoted to improving the steady-state accuracy of robot joints, while less considering the transient response constraints of the system. In order to make the joint response better close to the desired dynamic performance, Bechlioulis et al.[14] proposed the concept of prescribed performance control (PPC). This method can design the minimum convergence rate and maximum overshoot of the system according to the expected dynamic performance. Moreover, the tracking error can be confined within the allowable range no matter whether there exists the unknown change of model parameters or not[15]. Although the traditional exponential performance function can adjust the convergence rate by changing the exponential parameters, it is still infinite time convergence in theory. Therefore, Liu et al.[16] proposed the concept of finite-time convergence prescribed performance function (FTPF), and gradually developed the improved exponential performance function[17-18], the sine performance function[19], the composite performance function[20] and other forms. PPC provides support for achieving higher performance flexible joint control. However, the existing performance function still has problems such as complex solution, many control parameters and small adjustable range.

Backstepping control has advantages in realizing robust control or adaptive control of systems with uncertainties and unknown disturbances[21-22]. However, the high-order derivative of the virtual control law is involved in the backstepping process, which is easy to cause differential explosion and noise accumulation. The tracking differentiator (TD)[23] effectively solves the problem of high order derivative of signal. TD uses integral instead of differential process, which can reduce the amount of calculation and solve the problem of phase lag in the traditional filtering process. It is considered to be one of the most effective tools for obtaining signal derivative. Chen et al.[24] applied TD in the backstepping controller, and proved that using the tracking differentiator to solve the derivative of the virtual control law is feasible. Although various tracking differentiators with better performance have been gradually developed in subsequent studies[25-27], the existing differentiators still cannot solve the contradiction between rapid convergence and convergence stability. When a fast convergence rate is needed, it may cause the oscillation of the convergence curve near the equilibrium point.

In this paper, a flexible joint backstepping control method based on unknown state estimator and improved tracking differentiator is proposed, and an improved finite-time convergence prescribed performance function is introduced into the control equation to constrain the transient and dynamic performance of the system response.

The proposed method has the following innovations: (1) A finite-time convergence prescribed performance function with exponential convergence (EFTPF) trend is designed. Compared with the traditional exponential presupposed performance function[15], EFTPF has finite-time convergence characteristics, and its convergence time is independent of the initial conditions, which can be arbitrarily given and set in advance. Compared with other FTPFs in

Refs.[16-20], the exponential convergence trend of EFTPF is more conducive to the constraint response overshoot, and its form is simpler and the control parameters are fewer.(2) An unknown state observer is designed to estimate model uncertainty and external disturbance of the joint system. Compared with the other disturbance observers[10,13], the observer designed in this paper only needs to know the nominal values of inertia and stiffness of the joint system to estimate the lumped disturbance, which reduces the model dependence.(3) A hybrid tracking differentiator based on improved Sigmoid function (ISTD) is designed to track the derivative of virtual control law. Compared with the existing tracking differentiator[23,25-27], ISTD can adjust the concavity and convexity of the tracking function near the equilibrium point, which is helpful to improve the convergence stability while maintaining the tracking speed.

Finally, based on the above innovative theory, the prescribed performance backstepping controller of the flexible joint system is designed, and the Lyapunov function is designed to prove the stability of the system. According to the stability analysis results, the joint trajectory error satisfies the performance constraint, and all signals of the closed-loop system satisfy the uniform boundedness.

1 Preliminaries and Problem Formulation

1.1 Useful technical lemmas and definitions

Definition 1[15] $\rho(t)$ is a continuous function defined on the positive real number field, if it satisfies the following two conditions: (1) $\rho(t)>0$ and $\dot{\rho}(t)\leqslant 0$; (2) $\lim\limits_{t\to\infty}\rho(t)=\rho_\infty>0$, $\rho(t)$ is called to be a performance function.

Lemma 1[28] For bounded initial conditions, if there exists a C^1 continuous and positive definite Lyapunov function $V(x)$ satisfying $\|\kappa_1\|\leqslant V(x)\leqslant\|\kappa_2\|$, such that $\dot{V}(x)\leqslant-\beta V(x)+\gamma$, where κ_1, κ_2: $R^n\to R$, are class K functions, and β and γ are two positive constants, the solution $x(t)$ is uniformly bounded.

Lemma 2[23] System Σ is shown as

$$\begin{cases}\dot{z}_1(t)=z_2(t)\\ \dot{z}_2(t)=f(z_1(t),z_2(t))\end{cases}$$

where z_1, z_2 are the state variables of Σ. Provided that the tracking function $f(\cdot)$ has a solution, if any solution of Σ satisfies $\lim\limits_{t\to\infty}z_1(t)=0$, $\lim\limits_{t\to\infty}z_2(t)=0$, then for any bounded measurable and integratable input signal $r(t)$ and any constant $T>0$, the system Σ_0 is shown as

$$\begin{cases}\dot{v}_1(t)=v_2(t)\\ \dot{v}_2(t)=R^2 f\left(v_1(t)-r(t),\dfrac{v_2(t)}{R}\right)\end{cases}$$

and it satisfies

$$\lim_{R\to\infty}\int_0^T\left|v_1(t)-r(t)\right|\mathrm{d}t=0$$

where time constant $R>0$, and v_1, v_2 are the state variables of the system Σ_0.

1.2 Problem formulation

Consider the flexible joint physical model shown in Fig.1, where n is the reduction ratio.

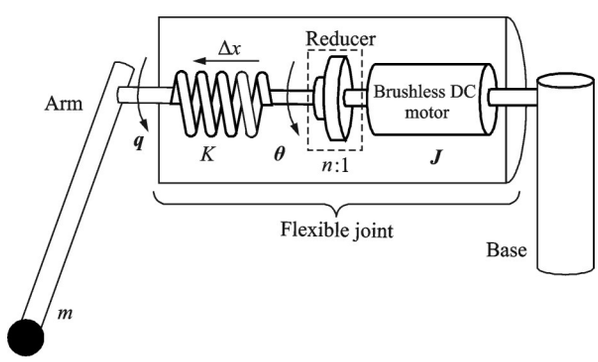

Fig.1 Physical model of single link flexible joint manipulator

The flexible joint dynamics model can be expressed as[29]

$$\begin{cases}\boldsymbol{I}\ddot{\boldsymbol{q}}+K(\boldsymbol{q}-\boldsymbol{\theta})+\dfrac{1}{2}mgl\sin(\boldsymbol{q})+\boldsymbol{\tau}_{f_l}+d_1=0\\ \boldsymbol{J}\ddot{\boldsymbol{\theta}}-K(\boldsymbol{q}-\boldsymbol{\theta})+\boldsymbol{\tau}_{f_m}+d_2=\boldsymbol{\tau}\end{cases}\tag{1}$$

where $\boldsymbol{q}$, $\dot{\boldsymbol{q}}$, $\ddot{\boldsymbol{q}}$ are the position, velocity, and acceleration vectors of the connecting rod, respectively; $\boldsymbol{\theta}$, $\dot{\boldsymbol{\theta}}$, $\ddot{\boldsymbol{\theta}}$ are the position, velocity, and acceleration vectors of the reducer, respectively; $mgl\sin(\boldsymbol{q})$ is the gravity term of the connecting rod; $\boldsymbol{I}$ and $\boldsymbol{J}$ are the rotational inertias of the connecting rod and the

joint motor, respectively; K is the joint stiffness; τ is the driving torque; τ_{f_l} and τ_{f_m} are the friction torques of connecting rod side and motor side, respectively; d_1 and d_2 are unknown external disturbances. The changes of load side mass, friction and joint stiffness are nonlinear terms that are difficult to accurately model. We can regard the sum of these nonlinear terms and external disturbances as lumped disturbances, and design observers to estimate the lumped disturbances. A lumped disturbance containing model uncertainties and external disturbances is defined as

$$\begin{cases}\delta_1 = \Delta I\ddot{q} + \Delta K(q-\theta) + \dfrac{1}{2}mgl\sin(q) + \tau_{f_l} + d_1 \\ \delta_2 = \Delta J\ddot{\theta} - \Delta K(q-\theta) + \tau_{f_m} + d_2\end{cases} \tag{2}$$

where Δ is the parameter uncertainty component. Therefore, Eq.(1) can be rewritten as

$$\begin{cases}I_m\ddot{q} + K_m(q-\theta) + \delta_1 = 0 \\ J_m\ddot{\theta} - K_m(q-\theta) + \delta_2 = \tau\end{cases} \tag{3}$$

where I_m, J_m and K_m are the nominal values of connecting rod inertia and motor inertia, and the joint stiffness coefficient, respectively. They satisfy $J = J_m + \Delta J$, $I = I_m + \Delta I$ and $K = K_m + \Delta K$.

Define $x_1 = q$, $x_2 = \dot{q}$, $x_3 = \theta$, $x_4 = \dot{\theta}$, and we can obtain the equation of state of the system as

$$\begin{cases}\dot{x}_1 = x_2 \\ \dot{x}_2 = -\dfrac{K_m(x_1 - x_3)}{I_m} - \dfrac{\delta_1}{I_m} \\ \dot{x}_3 = x_4 \\ \dot{x}_4 = \dfrac{K_m(x_1 - x_3)}{J_m} + \dfrac{\tau - \delta_2}{J_m} \\ y = x_1\end{cases} \tag{4}$$

where y is the output of the system.

To simplify the difficulty of the model analysis, the following assumptions are made.

Assumption 1 We only consider a single-joint flexible joint manipulator which can rotate in vertical plane. The connecting rod is rigid and the center of mass is at the center of the link.

Assumption 2 Assume that δ_1 and δ_2 and their derivatives are bounded, i.e there exists $h_i > 0$ and $g_i > 0$ such that $\|\delta_i\| \leqslant h_i$, $\|\dot{\delta}_i\| \leqslant g_i$, $i = 1, 2$.

The unmodeled perturbation in δ_i is a continuous bounded function of time. Although some studies have equivalent the friction term to the form of a switching function, this does not affect that the friction term is still a continuous function of time in actual joint motion. Therefore, Assumption 2 holds for unmodeled disturbances. The boundedness assumption of external unknown disturbances d_1 and d_2 is widely used in the design of disturbance observers, and the boundedness of external disturbances can be realized in practical robotic systems[30]. Therefore, Assumption 2 is reasonable and more realistic.

The control objective in this paper is to design a controller τ with a finite-time convergence performance function constraint for a flexible joint system (4) with model uncertainty and external disturbances, such that the joint output y rapidly and accurately tracks a continuous bounded desired trajectory y_d.

2 Design of Unknown State Estimator

In this section, a filter-based flexible joint unknown state estimator is designed to estimate the lumped disturbances δ_1 and δ_2. From Eq.(2), lumped disturbances include unknown nonlinear dynamic factors such as joint stiffness, the mass of connecting rod side, friction and external disturbances. From Eq.(3), we can reconstruct lumped perturbations δ_1 and δ_2 only using I_m, J_m, K_m and τ.

We first define the filtered variables x_{1f}, x_{2f}, x_{3f}, x_{4f} and τ_f with respect to x_1, x_2, x_3, x_4 and τ as

$$\begin{cases}k\dot{x}_{1f} + x_{1f} = x_1,\ x_{1f}(0) = 0 \\ k\dot{x}_{2f} + x_{2f} = x_2,\ x_{2f}(0) = 0 \\ k\dot{x}_{3f} + x_{3f} = x_3,\ x_{3f}(0) = 0 \\ k\dot{x}_{4f} + x_{4f} = x_4,\ x_{4f}(0) = 0 \\ k\dot{\tau}_f + \tau_f = \tau,\ \tau_f(0) = 0\end{cases} \tag{5}$$

where $k > 0$ is a filter parameter.

The low-pass filter in Eq.(5) aims to derive an invariant manifold for constructing the estimator without using the acceleration of joint.

Lemma 3 Consider system (4) with filtered variables defined in Eq.(5), then the manifold $Z_1 =$

$\frac{x_2-x_{2f}}{k}+\frac{K_m(x_{1f}-x_{3f})+\delta_1}{I_m}$ is an invariant manifold for any positive constant k, and $\lim_{k\to 0}\left\{\lim_{t\to\infty} Z_1(t)\right\}=0$ is true.

Proof Derivation of Z_1 is shown as

$$\dot{Z}_1=\frac{\dot{x}_2-\dot{x}_{2f}}{k}+\frac{K_m\left(\dot{x}_{1f}-\dot{x}_{3f}\right)}{I_m}+\frac{\dot{\delta}_1}{I_m}=\frac{1}{k}\left(\dot{x}_2-\frac{x_2-x_{2f}}{k}+\frac{K_m\left(x_1-x_{1f}-\left(x_3-x_{3f}\right)\right)}{I_m}+\frac{k\dot{\delta}_1}{I_m}\right)=\frac{1}{k}\left(-Z_1+\frac{k\dot{\delta}_1}{I_m}\right) \tag{6}$$

Select a Lyapunov function as $V_{Z_1}=Z_1^2/2$, such that

$$\dot{V}_{Z_1}=Z_1\frac{1}{k}\left(-Z_1+\frac{k\dot{\delta}_1}{I_m}\right)=-\frac{1}{k}Z_1^2+\frac{1}{I_m}Z_1\dot{\delta}_1 \tag{7}$$

According to the Young's inequality and Assumption 2, we have

$$Z_1\frac{\dot{\delta}_1}{I_m}\leqslant\frac{1}{2k}Z_1^2+\frac{k}{2}\frac{\dot{\delta}_1^2}{I_m^2}\leqslant\frac{1}{2k}Z_1^2+\frac{k}{2I_m^2}g_1^2 \tag{8}$$

So, there are

$$\dot{V}_{Z_1}\leqslant-\frac{1}{k}Z_1^2+\frac{1}{2k}Z_1^2+\frac{k}{2I_m^2}g_1^2=-\frac{1}{k}V_{Z_1}+\frac{k}{2I_m^2}g_1^2 \tag{9}$$

Solving Eq.(9) yields $V_{Z_1}\leqslant\exp(-t/k)V_{Z_1}(0)+\frac{k^2}{2I_m^2}g_1^2$, which indicated that $V_{Z_1}(t)$ and $Z_1(t)$ are all bounded, and $Z_1(t)$ will exponentially converge to a residual set defined as

$$\|Z_1\|=\sqrt{2V_{Z_1}}\leqslant\sqrt{\exp(-t/k)Z_1^2(0)+\frac{k^2}{I_m^2}g_1^2} \tag{10}$$

From Eq.(10), g_1 and k jointly determine the upper bound of Z_1 with $\lim_{k\to 0}\left\{\lim_{t\to\infty} Z_1(t)\right\}=0$, which indicates that $Z_1=0$ is an invariant manifold.

Lemma 4 Consider system (4) with filtered variables defined in Eq.(5), then the manifold $Z_2=\frac{x_4-x_{4f}}{k}-\frac{K_m\left(x_{1f}-x_{3f}\right)+\left(\tau_f-\delta_2\right)}{J_m}$ is an invariant manifold for any positive constant k, and $\lim_{k\to 0}\left\{\lim_{t\to\infty} Z_2(t)\right\}=0$ is true.

Proof Derivation of Z_2 is shown as

$$\dot{Z}_2=\frac{\dot{x}_4-\dot{x}_{4f}}{k}-\frac{K_m\left(\dot{x}_{1f}-\dot{x}_{3f}\right)+\left(\dot{\tau}_f-\dot{\delta}_2\right)}{J_m}=\frac{1}{k}\left(\dot{x}_4-\frac{x_4-x_{4f}}{k}-\frac{K_m\left(x_1-x_{1f}-\left(x_3-x_{3f}\right)\right)}{J_m}-\frac{\tau-\tau_f-k\dot{\delta}_2}{J_m}\right)=\frac{1}{k}\left(-Z_2+\frac{k\dot{\delta}_2}{J_m}\right) \tag{11}$$

Select a Lyapunov function as $V_{Z_2}=Z_2^2/2$, such that

$$\dot{V}_{Z_2}=Z_2\frac{1}{k}\left(-Z_2+\frac{k\dot{\delta}_2}{J_m}\right)=-\frac{1}{k}Z_2^2+Z_2\frac{\dot{\delta}_2}{J_m}\leqslant-\frac{1}{k}Z_2^2+\frac{1}{2k}Z_2^2+\frac{k}{2J_m^2}\dot{\delta}_2^2\leqslant-\frac{1}{k}V_{Z_2}+\frac{k}{2J_m^2}g_2^2 \tag{12}$$

Solving Eq.(12) yields $V_{Z_2}\leqslant\exp(-t/k)V_{Z_2}(0)+\frac{k^2}{2J_m^2}g_2^2$, which indicated that $V_{Z_2}(t)$ and $Z_2(t)$ are all bounded, and $Z_2(t)$ will exponentially converge to a residual set defined as

$$\|Z_2\|=\sqrt{2V_{Z_2}}\leqslant\sqrt{\exp(-t/k)Z_2^2(0)+\frac{k^2}{J_m^2}g_2^2} \tag{13}$$

From Eq.(13), g_2 and k jointly determine the upper bound of Z_2 with $\lim_{k\to 0}\left\{\lim_{t\to\infty} Z_2(t)\right\}=0$, which indicates that $Z_2=0$ is an invariant manifold.

According to Lemmas 3, 4, $Z_i=0$ ($i=1, 2$) holds when $k\to 0$, we can design the following unknown dynamic estimator as

$$\begin{cases}\hat{\delta}_1=-K_m\left(x_{1f}-x_{3f}\right)-\frac{I_m}{k}\left(x_2-x_{2f}\right)\\ \hat{\delta}_2=\tau_f-\frac{J_m}{k}\left(x_4-x_{4f}\right)+K_m\left(x_{1f}-x_{3f}\right)\end{cases} \tag{14}$$

If the low-pass filter $1/(ks+1)$ is applied to both sides of the second and fourth equations in Eq.(4), we can obtain

$$\begin{cases}\dot{x}_{2f}=-\frac{K_m(x_{1f}-x_{3f})}{I_m}-\frac{\delta_{1f}}{I_m}\\ \dot{x}_{4f}=\frac{K_m(x_{1f}-x_{3f})}{J_m}+\frac{\tau_f-\delta_{2f}}{J_m}\end{cases} \tag{15}$$

where δ_{1f} and δ_{2f} are filtered versions of δ_1 and δ_2, which are given by

$$\begin{cases}k\dot{\delta}_{1f}+\delta_{1f}=\delta_1\\ k\dot{\delta}_{2f}+\delta_{2f}=\delta_2\end{cases} \tag{16}$$

From Eqs.(14, 15), we can obtain: $\hat{\delta}_1=\delta_{1f}$,

$\hat{\delta}_2 = \delta_{2f}$. In this case, we can verify that $\dot{\tilde{\delta}}_1 = \dot{\delta}_{1f} = \frac{\delta_1 - \delta_{1f}}{k} = \frac{\delta_1 - \hat{\delta}_1}{k}$, $\dot{\tilde{\delta}}_2 = \dot{\delta}_{2f} = \frac{\delta_2 - \delta_{2f}}{k} = \frac{\delta_2 - \hat{\delta}_2}{k}$. If the error of the estimator is defined as $\tilde{\delta}_i = \delta_i - \hat{\delta}_i$, the derivative of the error is expressed as

$$\begin{cases} \dot{\tilde{\delta}}_1 = \dot{\delta}_1 - \dot{\tilde{\delta}}_1 = -\frac{1}{k}\tilde{\delta}_1 + \dot{\delta}_1 \\ \dot{\tilde{\delta}}_2 = \dot{\delta}_2 - \dot{\tilde{\delta}}_2 = -\frac{1}{k}\tilde{\delta}_2 + \dot{\delta}_2 \end{cases} \tag{17}$$

Theorem 1 Consider system (1) with estimator (14) for lumped uncertainties δ_i, then the estimation error $\tilde{\delta}_i$ is bounded by

$$\begin{cases} \left\| \tilde{\delta}_1 \right\| \leqslant \sqrt{\exp\left(-\frac{t}{k}\right)\delta_1^2(0) + k^2 g_1^2} \\ \left\| \tilde{\delta}_2 \right\| \leqslant \sqrt{\exp\left(-\frac{t}{k}\right)\delta_2^2(0) + k^2 g_2^2} \end{cases} \tag{18}$$

so that $\hat{\delta}_i \to \delta_i$ hold for $k \to 0$ or $g_i \to 0$.

Proof Take $\tilde{\delta}_1$ for example, select a Lyapunov function as $V_{\tilde{\delta}_1} = \tilde{\delta}_1^2/2$, and get its derivative as

$$\dot{V}_{\tilde{\delta}_1} = \tilde{\delta}_1 \dot{\tilde{\delta}}_1 = \tilde{\delta}_1\left(-\frac{1}{k}\tilde{\delta}_1 + \dot{\delta}_1\right) \leqslant -\frac{1}{k}\tilde{\delta}_1^2 + \frac{1}{2k}\tilde{\delta}_1^2 + \frac{k}{2}\dot{\delta}_1^2 \leqslant -\frac{1}{k}V_{\tilde{\delta}_1} + \frac{k}{2}g_1^2 \tag{19}$$

Solving Eq.(19), we can obtain $V_{\tilde{\delta}_1} \leqslant \exp(-t/k)V_{\tilde{\delta}_1}(0) + k^2 g_1^2/2$. Further known that $\left\| \tilde{\delta}_1 \right\| = \sqrt{2V_{\tilde{\delta}_1}} \leqslant \sqrt{\exp(-t/k)\tilde{\delta}_1^2(0) + k^2 g_1^2}$, and when $k \to 0$, $\hat{\delta}_1 \to \delta_1$.

Similarly, if we select $V_{\tilde{\delta}_2} = \tilde{\delta}_2^2/2$, we can obtain: $\left\| \tilde{\delta}_2 \right\| = \sqrt{2V_{\tilde{\delta}_2}} \leqslant \sqrt{\exp(-t/k)\tilde{\delta}_2^2(0) + k^2 g_2^2}$, and when $k \to 0$, $\hat{\delta}_2 \to \delta_2$.

Remark 1 The unknown state observer shown in Eq.(14) only needs to know the nominal values of joint inertia and stiffness, which reduces the dependence on nonlinear model parameters such as load side mass and friction torque. Moreover, the Eq.(14) does not need to obtain the acceleration signal of the system, which reduces the influence of signal noise. Therefore, the estimator designed in this paper is easier to implement in actual control.

Remark 2 The filtering parameter k determines the estimation error of the estimator and the sensitivity of the estimator to noise[13]. Usually, k is taken as a small constant to reduce the estimation error.

3 Finite-Time Performance Function

According to Definition 1, give the definition of a performance function with finite time convergence.

Definition 2[16] A smooth function $\rho(t)$ is called FTPF if it satisfies the following properties: (1) $\rho(t) > 0$ and $\dot{\rho}(t) \leqslant 0$; (2) $\lim\limits_{t \to T_1} \rho(t) = \rho_\infty$ which is an arbitrarily small positive number; (3) $\rho(t) = \rho_\infty$ for any $t \geqslant T_1$ with T_1 being the settling time.

According to Definition 2, an EFTPF is proposed by setting T_1 as the preset convergence time parameter

$$\rho(t) = \begin{cases} (\rho_0 - \rho_\infty)\left(\frac{1}{T_1^2}t^2 - \frac{2}{T_1}t + 1\right)^\alpha + \rho_\infty & 0 \leqslant t < T_1 \\ \rho_\infty & t \geqslant T_1 \end{cases} \tag{20}$$

where $\alpha \geqslant 1$ is the convergence coefficient; $\rho_0 = \rho(0)$, $\rho_\infty = \lim\limits_{t \to T_1} \rho(t)$ are the initial value and stable value of the performance function, respectively, and satisfy $\rho_0 > 2\rho_\infty > 0$.

Remark 3 The EFTPF (1) satisfies all properties in Definition 2, that is, $\rho(t)$ can converge to ρ_∞ within a given time T_1. Furthermore, the reason why $\alpha \geqslant 1$ is to ensure that EFTPF is a concave function, which will help to suppress overshoot.

In order to constrain the joint tracking error in a predetermined range, let $e = y - y_d$, and define the following inequality constraints

$$-\rho(t) < e(t) < \rho(t) \tag{21}$$

Under the constraints of boundary $\rho(t)$ and $-\rho(t)$, the error $e(t)$ will converge with the convergence speed of the prescribed performance function.

Remark 4 In contrast to the existing exponential performance function $\psi(t) = (\psi_0 - \psi_\infty)e^{-\sigma t} + \psi_\infty$[15], Eq.(20) has the performance of finite-time

convergence. Meanwhile, it can be seen from Definition 2 and Eq.(21) that EFTPF still makes $e(t)$ possess the predefined transient and steady-state performances.

Remark 5 Compared with[16]

$$\xi(t)=\begin{cases}\left(\xi_0^{\eta}-\lambda\eta t\right)^{\frac{1}{\eta}}+\xi_\infty & 0\leqslant t<T_1\\ \xi_\infty & t\geqslant T_1\end{cases}$$

Eq.(20) needs fewer parameters to be tuned and has simpler structure. In $\xi(t)$, the convergence time is calculated by $T_1=\xi_0^{\eta}/\eta\lambda$, and $\eta=q/p\in(0,1]$ with p and q defined as any positive odd and even integer, respectively. Therefore, when we need to change the constraint conditions of system response, we need to calculate the appropriate parameters p, q and λ first.

Remark 6 In contrast with[19]

$$\vartheta(t)=\begin{cases}(\vartheta_0-\vartheta_\infty)\left(\dfrac{\sin(2\pi t/T_1)}{2\pi}-\dfrac{t}{T_1}\right)+\vartheta_0 & 0\leqslant t<T_1\\ \vartheta_\infty & t\geqslant T_1\end{cases}$$

Eq.(20) has the ability to adjust the decline rate of performance function. In $\rho(t)$, the greater the value of α, the faster the decline rate of performance function, which helps to suppress system overshoot. In $\vartheta(t)$, however, $\vartheta(t)$ is a convex function when $t\to 0$, which is not conducive to suppressing system overshoot.

Remark 7 Compared with[20]

$$\dot{\varphi}(t)=\begin{cases}-\dfrac{\left(\varphi_0-\varphi_\infty\right)^{1-\kappa}}{(1-\kappa)T_1}\left(\varphi(t)-\varphi_\infty\right)^{\kappa} & 0\leqslant t<T_1\\ \varphi_\infty & t\geqslant T_1\end{cases}$$

$\varphi(t)$ and Eq.(20) have similar exponential convergence characteristics and the same finite time convergence ability. However, the proposed design process of Eq.(20) is simpler, because $\varphi(t)$ require either $\dot{V}(x)+b(V(x))^{\kappa}\leqslant 0, x\in P$ with $b>0$ and $\kappa\in(0,1)$, and $P\subseteq D$ is an open neighborhood of the origin[31]. In addition, the expression of $\varphi(t)$ is given by the solution of differential equation, while Eq.(20) avoids the process of solving differential equation.

In order to simplify the difficulty of control law design, inequality constraints of Eq.(21) can be transformed to equality constraints. The errors are transformed as follows

$$l(\varepsilon_1(t))=\frac{e(t)}{\rho(t)} \tag{22}$$

where $\varepsilon_1(t)$ is a transformed error; $l(\varepsilon_1(t))$ a function about the transformed error, which needs to satisfy the following conditions besides smooth, reversible and strictly increasing

$$\lim_{\varepsilon_1\to-\infty} l(\varepsilon_1(t))=-1,\ \lim_{\varepsilon_1\to+\infty} l(\varepsilon_1(t))=1 \tag{23}$$

In order to meet the above conditions, $l(\varepsilon_1)$ can be taken as

$$l(\varepsilon_1)=\frac{e^{\varepsilon_1}-e^{-\varepsilon_1}}{e^{\varepsilon_1}+e^{-\varepsilon_1}} \tag{24}$$

Because $l(\varepsilon_1)$ is reversible, the transformed error $\varepsilon_1(t)$ can be expressed as

$$\varepsilon_1(t)=l^{-1}\left(\frac{e(t)}{\rho(t)}\right)=\frac{1}{2}\ln\frac{e(t)+\rho(t)}{\rho(t)-e(t)} \tag{25}$$

The derivative of $\varepsilon_1(t)$ is

$$\dot{\varepsilon}_1(t)=\frac{\mathrm{d}l^{-1}}{\mathrm{d}t}=\frac{1}{2}\frac{\rho(t)-e(t)}{e(t)+\rho(t)}\left(\frac{e(t)+\rho(t)}{\rho(t)-e(t)}\right)'=\frac{\dot{e}(t)\rho(t)-e(t)\dot{\rho}(t)}{\rho^2(t)-e^2(t)}=\Gamma(e,\rho)\left(\dot{e}(t)-\frac{e(t)\dot{\rho}(t)}{\rho(t)}\right) \tag{26}$$

where $\Gamma(e,\rho)=\dfrac{\rho}{\rho^2-e^2}$.

The nature of PPC is barrier function based control, and thus whenever the error approaches the boundary function, the control input would be large enough to suppress the error[32]. Therefore, as long as the actuator does not fall into saturation, there will be no singular problem in Eq.(25). At the same time, it is also necessary to select the performance function parameters according to the actual performance of the controlled object to avoid the actuator saturation problem.

4 Controller Design

4.1 Prescribed performance-based backstepping controller

In order to enable the flexible joint to track the

desired trajectory quickly and accurately, and meet the performance function constraints, this section will design a backstepping controller based on the conversion error. The detailed steps are as follows.

Step 1 Construct Lyapunov function V_1

$$V_1=\frac{1}{2}\varepsilon_1^2 \tag{27}$$

There is

$$\dot{V}_1=\varepsilon_1\dot{\varepsilon}_1=\varepsilon_1\Gamma\left(\dot{x}_1-\dot{y}_d-\frac{e\dot{\rho}}{\rho}\right)=$$
$$\varepsilon_1\Gamma\left(\varepsilon_2+\lambda_1-\dot{y}_d-\frac{e\dot{\rho}}{\rho}\right) \tag{28}$$

Let $\varepsilon_2=x_2-\lambda_1$, and taking the virtual control law λ_1 as

$$\lambda_1=\dot{y}_d+\frac{e\dot{\rho}}{\rho}-k_1\Gamma^{-1}\varepsilon_1 \tag{29}$$

where k_1 is a constant greater than 0. Eq.(28) may be rewritten as

$$\dot{V}_1=\varepsilon_1\dot{\varepsilon}_1=-k_1\varepsilon_1^2+\varepsilon_1\Gamma\varepsilon_2 \tag{30}$$

Step 2 Construct Lyapunov function V_2

$$V_2=V_1+\frac{1}{2}I_m\varepsilon_2^2 \tag{31}$$

There is

$$\dot{V}_2=\dot{V}_1+I_m\varepsilon_2\dot{\varepsilon}_2=$$
$$\dot{V}_1+I_m\varepsilon_2\frac{1}{I_m}\left(-K_m(x_1-x_3)-\delta_1-I_m\dot{\lambda}_1\right)=$$
$$\dot{V}_1+\varepsilon_2\left(-K_mx_1+K_m\varepsilon_3+K_m\lambda_2-\delta_1-I_m\dot{\lambda}_1\right) \tag{32}$$

Let $\varepsilon_3=x_3-\lambda_2$, and taking the virtual control law λ_2 as

$$\lambda_2=\frac{1}{K_m}\left(\hat{\delta}_1+I_m\dot{\bar{\lambda}}_1-k_2\varepsilon_2-\varepsilon_1\Gamma+K_mx_1\right) \tag{33}$$

where k_2 is a constant greater than 0; and $\dot{\bar{\lambda}}_1$ the estimated value of the first derivative of the virtual control law λ_1. Since the derivative process of λ_1 has the risk of differential explosion and noise interference, the derivative estimation value is used to replace the differential solution process.

According to Eq.(33), Eq.(32) can be rewritten to

$$\dot{V}_2=\dot{V}_1+I_m\varepsilon_2\dot{\varepsilon}_2=\dot{V}_1+K_m\varepsilon_2\varepsilon_3-\varepsilon_2\tilde{\delta}_1+$$
$$I_m\left(\dot{\bar{\lambda}}_1-\dot{\lambda}_1\right)\varepsilon_2-k_2\varepsilon_2^2-\varepsilon_1\varepsilon_2\Gamma \tag{34}$$

Substituting Eq.(30) into Eq.(34), with

$$\dot{V}_2=-k_1\varepsilon_1^2-k_2\varepsilon_2^2+K_m\varepsilon_2\varepsilon_3-\varepsilon_2\tilde{\delta}_1+I_m\left(\dot{\bar{\lambda}}_1-\dot{\lambda}_1\right)\varepsilon_2 \tag{35}$$

Step 3 Construct Lyapunov function V_3

$$V_3=V_2+\frac{1}{2}\varepsilon_3^2 \tag{36}$$

There is

$$\dot{V}_3=\dot{V}_2+\varepsilon_3\dot{\varepsilon}_3=\dot{V}_2+\varepsilon_3(x_4-\dot{\lambda}_2) \tag{37}$$

Let $\varepsilon_4=x_4-\lambda_3$, and taking the virtual control law λ_3 as

$$\dot{V}_3=\dot{V}_2+\varepsilon_3\dot{\varepsilon}_3=\dot{V}_2+\varepsilon_3(\varepsilon_4+\lambda_3-\dot{\lambda}_2) \tag{38}$$

To ensure system stability, the virtual control law λ_3 is

$$\lambda_3=-k_3\varepsilon_3+\dot{\bar{\lambda}}_2-K_m\varepsilon_2 \tag{39}$$

where k_3 is a constant greater than 0; and $\dot{\bar{\lambda}}_2$ the estimated value of the first derivative of the virtual control law λ_2.

Substituting Eqs.(35, 39) into Eq.(38), we have

$$\dot{V}_3=-k_1\varepsilon_1^2-k_2\varepsilon_2^2-k_3\varepsilon_3^2+\varepsilon_2I_m\left(\dot{\bar{\lambda}}_1-\dot{\lambda}_1\right)+$$
$$\varepsilon_3\left(\dot{\bar{\lambda}}_2-\dot{\lambda}_2\right)-\varepsilon_2\tilde{\delta}_1+\varepsilon_3\varepsilon_4 \tag{40}$$

Step 4 Construct Lyapunov function V_4

$$V_4=V_3+\frac{1}{2}J_m\varepsilon_4^2 \tag{41}$$

There is

$$\dot{V}_4=\dot{V}_3+J_m\varepsilon_4\dot{\varepsilon}_4=$$
$$\dot{V}_3+J_m\varepsilon_4\frac{1}{J_m}\left(K_m(x_1-x_3)+\tau-\delta_2-J_m\dot{\lambda}_3\right)=$$
$$\dot{V}_3+\varepsilon_4\left(\tau+K_m(x_1-x_3)-\delta_2-J_m\dot{\lambda}_3\right) \tag{42}$$

For $\dot{V}_4\leqslant 0$, the control law τ is designed to

$$\tau=-K_m(x_1-x_3)+J_m\dot{\bar{\lambda}}_3+\hat{\delta}_2-k_4\varepsilon_4-\varepsilon_3 \tag{43}$$

where k_4 is a constant greater than 0; and $\dot{\bar{\lambda}}_3$ the estimated value of the first derivative of the virtual control law λ_3.

Substituting Eqs.(40,43) into Eq.(42), with

$$\dot{V}_4=-k_1\varepsilon_1^2-k_2\varepsilon_2^2-k_3\varepsilon_3^2-k_4\varepsilon_4^2+\varepsilon_2I_m\left(\dot{\bar{\lambda}}_1-\dot{\lambda}_1\right)+$$
$$\varepsilon_3\left(\dot{\bar{\lambda}}_2-\dot{\lambda}_2\right)+\varepsilon_4J_m\left(\dot{\bar{\lambda}}_3-\dot{\lambda}_3\right)-\varepsilon_2\tilde{\delta}_1-\varepsilon_4\tilde{\delta}_2 \tag{44}$$

Virtual control law Eqs.(29, 33, 39) and joint torque control Eq.(43) constitute the control equations of flexible joint system constrained by performance function. Among them, larger controller

gains k_1, k_2, k_3 and k_4 can improve the convergence speed, but also increase the control torque[33]. Therefore, the selection of control gain needs to consider the constraint performance and control torque.

4.2 Design of a hybrid differentiator based on an improved Sigmoid function

According to Eqs. (29, 33, 39, 43), the back-stepping controller contains the high-order derivative term of the virtual control law, which makes the controller have the problems of differential explosion and noise superposition. In order to solve this problem, a tracking differentiator based on improved Sigmoid function is designed in this section to obtain the derivative of the virtual control law.

Lemma 2 shows that under the function $f(\cdot)$, the solution $v_1(t)$ of the system Σ will fully approximate the input signal $r(t)$ at any finite time T. If $\dot{v}_1(t)=v_2(t)$ is taken as the differential of the input signal $r(t)$, then $v_2(r,t)$ will also converge to the generalized differential of $r(t)$. Therefore, $f(\cdot)$ determines the global convergence and filtering ability of the tracking differentiator.

The Sigmoid function is monotonic, bounded and symmetric and is suitable for use as a tracking function for tracking differentiators. On the basis of ensuring the monotonicity, boundedness and symmetry of the Sigmoid function, an improved Sigmoid function is proposed by introducing magnitude factors and exponential factors

$$\mathrm{Sig}(v;a,b,c)=\mathrm{sgn}(v)\cdot\left|a[(1+e^{-bv})^{-1}-0.5]\right|^{c} \tag{45}$$

where a is a magnitude factor used to adjust the output amplitude; b and c are exponential factors to regulate the convergence properties near the equilibrium point, here $c=q/p$; p and q are positive odd numbers; $|\cdot|$ ensures that $\mathrm{Sig}(v)$ is meaningful over the domain of real numbers; and $\mathrm{sgn}(v)$ is a symbolic function of v and ensures that $\mathrm{Sig}(v)$ is an odd function about the equilibrium point. Fig.2 shows the curve of Eq.(45) when a, b and c take different values.

Remark 8 As can be seen from Fig.2, with the increase of parameter c, the Sig function changes from a convex function to a concave function near the equilibrium point, and the changing trend gradually slows down, but it still keeps a fast convergence rate at the place far from the equilibrium point. Compared with $\mathrm{sig}(v)=a[(1+e^{-bv})-1-0.5]$[34], the parameter c in Eq.(45) can effectively change the concave-convex property of the Sig function near the equilibrium point, and make the Sig function have the ability to approach 0^+ as a concave function. This means that the tracking differentiator based on Eq.(45) will have both high-speed tracking ability and high convergence stability.

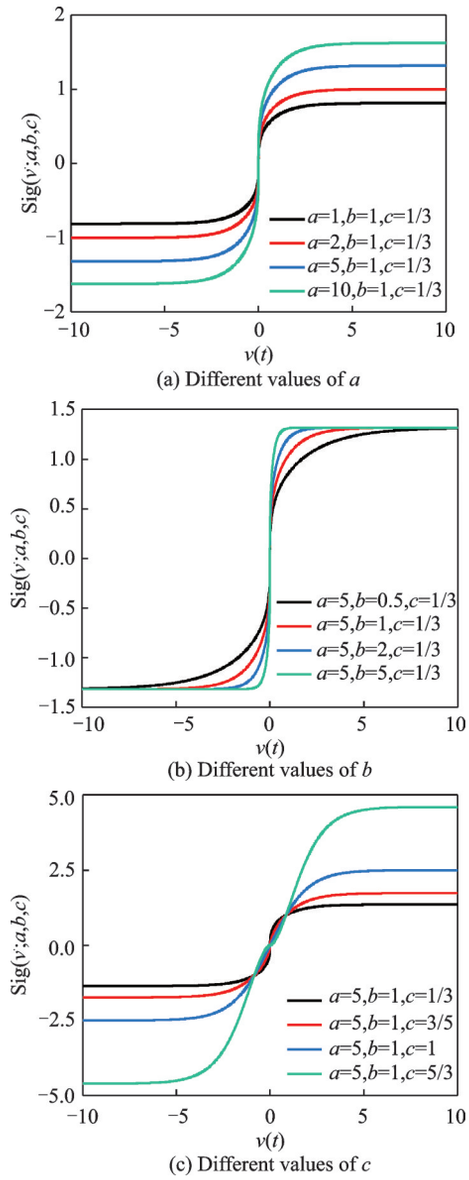

Fig.2 Curves of improved Sig(v) function with different parameters

In order to keep a high convergence speed of

state variables in the whole real number field, a hybrid system combining linear and non-linear is designed.

Theorem 2 Design system Σ_1 as

$$\begin{cases}\dot{z}_1(t)=z_2(t)\\ \dot{z}_2(t)=-z_1(t)-\mathrm{Sig}(z_1(t);a_1,b_1,c_1)-\\ \qquad z_2(t)-\mathrm{Sig}(z_2(t);a_2,b_2,c_2)\end{cases}\tag{46}$$

If a_1, b_1, a_2, and b_2 are all positive numbers greater than zero, and p and q are positive odd numbers, then the system Σ_1 satisfies the Lyapunov asymptotic stability condition, i.e.

$$\lim_{t\to\infty}z_1(t)=0,\lim_{t\to\infty}z_2(t)=0$$

Proof Construct the Lyapunov function as

$$V(z_1,z_2)=\int_0^{z_1}\mathrm{Sig}\left(\xi;a_1,b_1,c_1\right)\mathrm{d}\xi+\frac{1}{2}z_2^2+\frac{1}{2}z_1^2\tag{47}$$

Since $\mathrm{Sig}(x)$ is an odd function, z_1 is the same sign as $\mathrm{Sig}(x)$ when $z_1\neq0$, so by the definite integral property we have

$$\int_0^{z_1}\mathrm{Sig}\left(\xi;a_1,b_1,c_1\right)\mathrm{d}\xi>0$$

Clearly $V(z_1,z_2)>0$. Taking the derivative of Eq. (47), we have

$$\begin{aligned}\dot{V}(z_1,z_2)&=\mathrm{Sig}(z_1;a_1,b_1,c_1)z_2+z_2\dot{z}_2+z_1z_2=\\ &\mathrm{Sig}(z_1;a_1,b_1,c_1)z_2+z_2(-z_1-\mathrm{Sig}(z_1;a_1,b_1,c_1)-\\ &z_2-\mathrm{Sig}(z_2;a_2,b_2,c_2))z_1z_2=\\ &-z_2^2-z_2\mathrm{Sig}(z_2;a_2,b_2,c_2)\leqslant0\end{aligned}\tag{48}$$

When $\dot{V}(z_1,z_2)=0$, it can be concluded that $z_2=0$ and $\dot{z}_2=0$ from Eq.(48), and further, $z_1=0$ and $\dot{z}_1=0$ from Eq.(46). Therefore, the system Σ_1 is asymptotically stable with (0,0) as the equilibrium point, that is, when $t\to\infty$, we have $z_1\to0$, $z_2\to0$.

According to Lemma 2 and Theorem 1, design a hybrid tracking differentiator based on an improved Sigmoid function.

Theorem 3 Design system Σ_2 as

$$\begin{cases}\dot{v}_1(t)=v_2(t)\\ \dot{v}_2(t)=R^2\left\{-(v_1(t)-r(t))-\mathrm{Sig}(v_1(t)-\right.\\ \qquad\left.r(t))-\dfrac{v_2(t)}{R}-\mathrm{Sig}\left(\dfrac{v_2(t)}{R}\right)\right\}\\ y_{\Sigma_2}=v_1(t)\end{cases}\tag{49}$$

If a_1, b_1, a_2, b_2 and R are all positive numbers greater than zero, and p_1, q_1, p_2 and q_2 are positive odd numbers, then for any bounded measurable, integratable input signal $r(t)$ and any $T>0$, it satisfies

(1) $\lim\limits_{R\to\infty}\int_0^T\left|v_1(t)-r(t)\right|\mathrm{d}t=0$;

(2) Σ_2 is a perturbation form of Σ_1.

Proof Since system Σ_2 and system Σ_0 have formal equivalence, it follows from Lemma 2 that conclusion (1) of Theorem 3 holds.

For the conclusion (2) of Theorem 3, note

$$e_1=v_1(t)-r(t),\ e_2=v_2(t)-\dot{r}(t)$$

then the error system for the signal $r(t)$ is expressed as

$$\begin{cases}\dot{e}_1=e_2\\ \dot{e}_2=-R^2\left[e_1+\mathrm{Sig}(e_1)+\dfrac{e_2+\dot{r}(t)}{R}+\right.\\ \qquad\left.\mathrm{Sig}\left(\dfrac{e_2+\dot{r}(t)}{R}\right)\right]-\ddot{r}(t)\end{cases}\tag{50}$$

that is

$$\begin{cases}\dfrac{\mathrm{d}e_1}{\mathrm{d}Rt}=\dfrac{e_2}{R}\\ \dfrac{\mathrm{d}(e_2/R)}{\mathrm{d}Rt}=-\left[e_1+\mathrm{Sig}(e_1)+\dfrac{e_2+\dot{r}(t)}{R}+\right.\\ \qquad\left.\mathrm{Sig}\left(\dfrac{e_2+\dot{r}(t)}{R}\right)\right]-\dfrac{\ddot{r}(t)}{R^2}\end{cases}\tag{51}$$

If we take $\tau=Rt$, $z_1(\tau)=e_1(t)$, $z_2(\tau)=e_2(t)/R$, $z=[z_1,z_2]^{\mathrm{T}}$, Eq.(50) can be written as

$$\begin{cases}\dfrac{\mathrm{d}z_1}{\mathrm{d}\tau}=z_2\\ \dfrac{\mathrm{d}z_2}{\mathrm{d}\tau}=-\left[z_1+\mathrm{Sig}(z_1)+(z_2+\dfrac{\dot{r}(t)}{R})+\right.\\ \qquad\left.\mathrm{Sig}\left(z_2+\dfrac{\dot{r}(t)}{R}\right)\right]-\dfrac{\ddot{r}(t)}{R^2}\end{cases}\tag{52}$$

where $\lim\limits_{R\to\infty}\dot{r}(t)/R=0$ and $\lim\limits_{R\to\infty}\ddot{r}(t)/R=0$.

At this point, Eq.(52) is equivalent to the system Σ_1, and also has global zero asymptotic stability. Therefore, Σ_2 is a perturbation form of Σ_1, and Theorem 3 is proved.

Remark 9 The system Σ_2 is a hybrid tracking differentiator based on the improved Sigmoid function (ISTD), which can select appropriate R, a, b, and c according to the desired dynamic characteristics. It is worth noting that the larger R value can improve the tracking speed, but it will re-

duce the noise suppression ability of the tracking differentiator. The increase of c will be beneficial to the smooth convergence of the tracking differentiator, but the excessive value of c will also reduce the convergence rate. Therefore, the values of R and c should not be too large, and should be adjusted according to the expected tracking performance.

Remark 10 If the state variables v_1 and v_2 in ISTD are respectively corresponding to the virtual control law λ_i and its derivative $\dot{\lambda}_i$ ($i=1, 2, 3$), ISTD can effectively approximate the first derivative of any virtual control law. The advantage of doing so is to avoid the differential explosion problem in the derivation process and suppress the signal noise.

4.3 Stability analysis

Select a Lyapunov function

$$V_s = V_4 + \frac{1}{2}\tilde{\delta}_1^2 + \frac{1}{2}\tilde{\delta}_2^2 \tag{53}$$

then calculate its derivative along Eq.(53) as

$$\begin{aligned}\dot{V}_s = {} & \dot{V}_4 + \tilde{\delta}_1\dot{\tilde{\delta}}_1 + \tilde{\delta}_2\dot{\tilde{\delta}}_2 = \\ & -k_1\varepsilon_1^2 - k_2\varepsilon_2^2 - k_3\varepsilon_3^2 - k_4\varepsilon_4^2 + \varepsilon_2 I_m\left(\dot{\tilde{\lambda}}_1 - \dot{\lambda}_1\right) + \\ & \varepsilon_3\left(\dot{\tilde{\lambda}}_2 - \dot{\lambda}_2\right) + \varepsilon_4 J_m\left(\dot{\tilde{\lambda}}_3 - \dot{\lambda}_3\right) - \varepsilon_2\tilde{\delta}_1 - \varepsilon_4\tilde{\delta}_2 + \\ & \tilde{\delta}_1\dot{\tilde{\delta}}_1 + \tilde{\delta}_2\dot{\tilde{\delta}}_2\end{aligned} \tag{54}$$

The tracking error of tracking differentiator can be controlled within a certain range, that is, there is a normal number ς_i, satisfying[35]

$$\left|\dot{\tilde{\lambda}}_i - \dot{\lambda}_i\right| \leqslant \varsigma_i \quad i = 1, 2, 3 \tag{55}$$

According to the Young's inequality[36]

$$\begin{cases}\varepsilon_2 I_m\left(\dot{\tilde{\lambda}}_1 - \dot{\lambda}_1\right) \leqslant \dfrac{1}{2}I_m^2\varsigma_1^2 + \dfrac{1}{2}\varepsilon_2^2 \\ \varepsilon_3\left(\dot{\tilde{\lambda}}_2 - \dot{\lambda}_2\right) \leqslant \dfrac{1}{2}\varsigma_2^2 + \dfrac{1}{2}\varepsilon_3^2 \\ \varepsilon_4 J_m\left(\dot{\tilde{\lambda}}_3 - \dot{\lambda}_3\right) \leqslant \dfrac{1}{2}J_m^2\varsigma_3^2 + \dfrac{1}{2}\varepsilon_4^2 \\ -\varepsilon_2\tilde{\delta}_1 \leqslant \dfrac{1}{2}\varepsilon_2^2 + \dfrac{1}{2}\tilde{\delta}_1^2 \\ -\varepsilon_4\tilde{\delta}_2 \leqslant \dfrac{1}{2}\varepsilon_4^2 + \dfrac{1}{2}\tilde{\delta}_2^2\end{cases} \tag{56}$$

Substituting Eq.(19) and Eq.(56) into Eq.(54), we can obtain

$$\begin{aligned}\dot{V}_s \leqslant {} & -k_1\varepsilon_1^2 - (k_2-1)\varepsilon_2^2 - \left(k_3 - \frac{1}{2}\right)\varepsilon_3^2 - (k_4-1)\varepsilon_4^2 - \\ & \left(\frac{1}{2k} - \frac{1}{2}\right)\tilde{\delta}_1^2 - \left(\frac{1}{2k} - \frac{1}{2}\right)\tilde{\delta}_2^2 + \frac{1}{2}I_m^2\varsigma_1^2 + \frac{1}{2}J_m^2\varsigma_3^2 + \\ & \frac{1}{2}\varsigma_2^2 + \frac{k}{2}g_1^2 + \frac{k}{2}g_2^2\end{aligned} \tag{57}$$

According to Lemma 1, $\dot{V}_s$ can be expressed as

$$\dot{V}_s \leqslant -\beta V_s + \gamma \tag{58}$$

and β and γ are respectively expressed as

$$\begin{cases}\beta = \min\left[2k_1, \dfrac{1}{I_m}(2k_2-2), 2k_3-1, \dfrac{1}{J_m}(2k_4-2), \right. \\ \qquad \left. \dfrac{1}{k}-1, \dfrac{1}{k}-1\right] \\ \gamma = \dfrac{1}{2}I_m^2\varsigma_1^2 + \dfrac{1}{2}J_m^2\varsigma_3^2 + \dfrac{1}{2}\varsigma_2^2 + \dfrac{k}{2}g_1^2 + \dfrac{k}{2}g_2^2\end{cases} \tag{59}$$

where, to satisfy $\beta>0$, take $k_1>0$, $k_2>1$, $k_3>1/2$, $k_4>1$, $k<1$.

Solving the inequality (58), one can easily verify that

$$\begin{aligned}0 \leqslant V_s(t) \leqslant {} & V_s(0)\exp(-\beta t) + \frac{\gamma}{\beta}\left(1 - \right. \\ & \left.\exp(-\beta t)\right)\end{aligned} \tag{60}$$

Further, by Eq.(53) and Eq.(60), we have

$$V_1 \leqslant V_s \leqslant V_s(0)\exp(-\beta t) + \frac{\gamma}{\beta}\left(1 - \exp(-\beta t)\right) \tag{61}$$

that is

$$\begin{aligned}\frac{1}{2}\varepsilon_1^2 \leqslant {} & V_s(0)\exp(-\beta t) + \frac{\gamma}{\beta}\left(1 - \exp(-\beta t)\right) \leqslant \\ & V_s(0)\exp(-\beta t) + \frac{\gamma}{\beta}\end{aligned} \tag{62}$$

Substituting Eq.(25) into Eq.(62), there is

$$\begin{aligned}\frac{1}{2}\left(\frac{1}{2}\ln\frac{e+\rho}{\rho-e}\right)^2 \leqslant {} & V_s(0)\exp(-\beta t) + \frac{\gamma}{\beta} \leqslant \\ & V_s(0) + \frac{\gamma}{\beta}\end{aligned} \tag{63}$$

Solving the inequality (63), it can be obtained as

$$|e| \leqslant \frac{\exp\left(\left(8V_s(0) + \dfrac{8\gamma}{\beta}\right)^{\frac{1}{2}}\right) - 1}{\exp\left(\left(8V_s(0) + \dfrac{8\gamma}{\beta}\right)^{\frac{1}{2}}\right) + 1}|\rho| < |\rho| \tag{64}$$

According to Eq.(64), under the combined ac-

tion of virtual control laws (29, 33, 39) and controller (43), joint tracking error always satisfies the boundary constraint of performance function, namely $e\in(-\rho,\rho)$.

Remark 1 According to Eq.(60), when $t\to\infty$, V_s is bounded, and further according to Eq.(53), $\varepsilon_{1,2,3,4}$ and $\tilde{\delta}_{1,2}$ are also uniformly bounded. Because the desired trajectory y_d and its derivatives are bounded, we can deduce that $x_i\,(i=1,2,3,4)$ is bounded from the boundedness of $\varepsilon_{1,2,3,4}$. Further, according to Eq.(43), the control equation τ is also bounded. Therefore, under the combined action of virtual control laws (29, 33, 39) and controller (43), all closed-loop signals are uniformly ultimately bounded.

5 Simulation Analysis

In this section, the effectiveness and superiority of the proposed method are verified by simulation.

Firstly, in order to reflect the improvement of the prescribed performance function designed in this paper, we compared several performance function curves mentioned in Remarks 4—7. Taking $T_1=4$ s, the parameters of each performance function are shown in Table 1 and the curves of each function are shown in Fig.3.From Fig.3, it can be seen that compared with the traditional exponential performance function $\psi(t)$, the performance function $\rho(t)$ designed in this paper has finite time convergence characteristics. Compared with $\vartheta(t)$, $\rho(t)$ can adjust the descent rate, and the concave function property of $\rho(t)$ can suppress the response overshoot more effectively. Compared with $\xi(t)$, $\rho(t)$ has fewer adjusting parameters and a simpler form. Compared with $\varphi(t)$, $\rho(t)$ avoids the process of solving differential equations. The convergence characteristics of each performance function are consistent with the description of Remarks 4—7 in the fourth part, which proves the advantages and correctness of the preset performance function designed in this paper.

Table 1 Parameter values for performance functions

Function	Parameter value
$\psi(t)$	$\psi_0=1,\psi_\infty=0.02,\sigma=0.6$
$\vartheta(t)$	$\vartheta_0=1,\vartheta_\infty=0.02$
$\xi(t)$	$\xi_0=1,\xi_\infty=0.02,\eta=0.5,\lambda=0.5$
$\varphi(t)$	$\varphi_0=1,\varphi_\infty=0.02,\kappa=0.6$
$\rho(t)$	$\rho_0=1,\rho_\infty=0.02,\alpha=2$

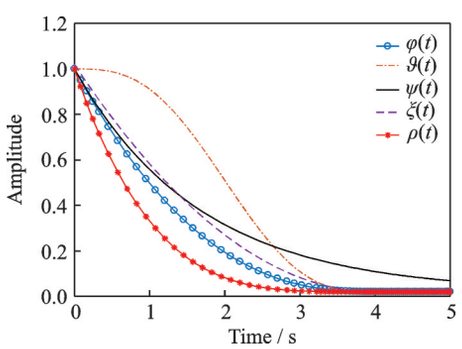

Fig.3 Comparison of performance function curves

To verify the effectiveness and advantage of the ISTD, the tracking performance of the ISTD is simulated and compared with a modified tracking differentiator with high stability and speed (MTD)[25] and a sliding mode tracking differentiator (SMTD)[37], using $\sin(t)$ as the input signal. MTD and SMTD are shown in Eqs.(65, 66), respectively. The parameter values are shown in Table 2.

MTD is shown as

$$\begin{cases}\dot{x}_1(t)=x_2(t)\\ \dot{x}_2(t)=-aR^2\left((x_1(t)-r(t))+\dfrac{x_2(t)}{R}\right)-\\ \qquad\qquad bR^2\left((x_1(t)-r(t))^m+\left(\dfrac{x_2(t)}{R}\right)^m\right)\end{cases}\tag{65}$$

SMTD is shown as

$$\begin{cases}\dot{x}_1(t)=x_2(t)-\lambda\left|x_1(t)-r(t)\right|^{\frac{1}{2}}\operatorname{sgn}(x_1(t)-r(t))\\ \dot{x}_2(t)=-\beta\operatorname{sgn}(x_1(t)-r(t))\end{cases}\tag{66}$$

Table 2 Parameter values for tracking differentiators

Differentiator	Parameter value
ISTD	$R=50,\ a_{1,2}=5,\ b_{1,2}=5,\ c_{1,2}=5/3$
MTD	$R=50,\ a=5,\ b=5,\ m=3$
SMTD	$\lambda=6,\ \beta=8$

The simulation results when tracking an ideal sinusoidal signal are shown in Fig.4. In Fig.4(a), all three differentiators can achieve effective tracking of the given signal. In Fig.4(b), SMTD has a more obvious oscillation near the equilibrium position, while the convergence of ISTD and MTD is relatively smooth. However, compared with MTD,

ISTD can estimate the differential signal within 0.04 s and the estimation results are closer to the ideal case. Therefore, ISTD has a faster response time and higher derivative accuracy.

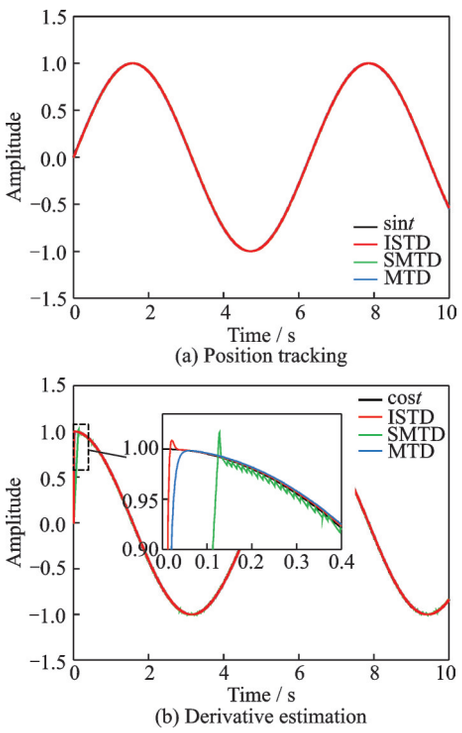

Fig. 4 Comparison of tracking performance of differentiators in the absence of noise

Adding random white noise with average amplitude of 0.05 and sampling time of 0.01 s to the input signal sin$t$. Comparing the filtering effect of the three differentiators, the results are shown in Fig.5. It can be seen in Fig.5 that all three differentiators have the ability to suppress signal noise, but ISTD suppression effect is better than MTD and SMTD, and the noise has the least effect on the differential estimation results.

Finally, to verify the effectiveness of the backstepping controller designed in this paper, we compared the control effects of the following methods.

Method 1 (M1) Eq.(14) is used as the unknown state estimator, Eqs.(29,33,39) are used as the virtual control law, and Eq.(43) is used as the controller. The parameters of the performance function $\rho(t)$ are: $\rho_0=1$, $\rho_\infty=0.02$, $\alpha=2$, $T_1=0.5$ s.

Method 2 (M2) Eq.(14) is used as the unknown state estimator. The function $\xi(t)$ in Remark

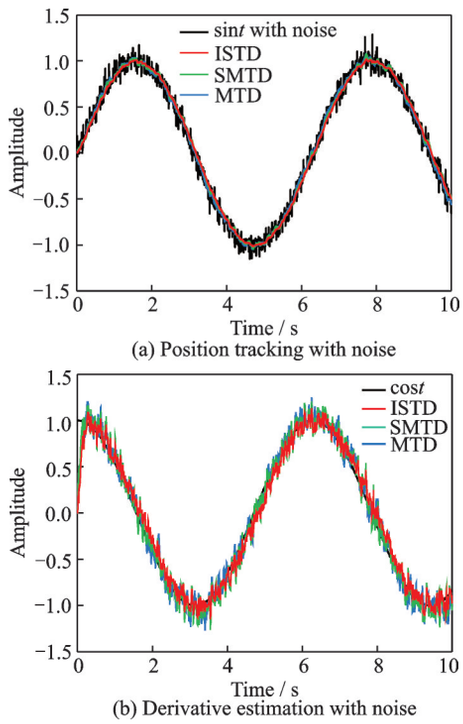

Fig.5 Comparison of tracking performance of differentiators in the presence of noise

5 is used as the prescribed performance function, and the inversion controller is designed according to the same method as in Section 4.1. The parameters of the performance function $\xi(t)$ are: $\xi_0=1$, $\xi_\infty=0.02$, $T_1=0.5$ s, $\eta=1$, $\lambda=2$.

Method 3 (M3) Eq.(14) is used as the unknown state estimator. The function $\psi(t)$ in Remark 4 is used as the prescribed performance function, and the inversion controller is designed according to the same method as in Section 4.1. The parameters of the performance function $\psi(t)$ are: $\psi_0=1$, $\psi_\infty=0.02$, $\sigma=2$.

Method 4 (M4) PD controller, where $K_P=10$, $K_D=10$.

The parameters of flexible joints are set as $I_m=0.45$ kg·m^2, $J_m=0.062$ kg·m^2, $K_m=15$ N·m/rad, $mgl=5$ N·m. The parameters of the virtual control law are $k_1=2$, $k_2=5$, $k_3=15$, $k_4=10$, and the filtering coefficient $k=0.01$. The unknown disturbance is set as

$$\begin{cases}\delta_1=0.1I_m\ddot{q}+0.1K_m(q-\theta)+\dfrac{1}{2}mgl\sin q+\\ \qquad 0.1\mathrm{sgn}(\dot{q})+0.1\sin t\\ \delta_2=0.1J_m\ddot{\theta}-0.1K_m(q-\theta)+0.1\mathrm{sgn}(\dot{\theta})+0.1\sin t\end{cases}$$

When the given trajectory is $\sin(2t)$, the simulation results are shown in Figs. 6—10. It can be seen from Figs. 6 and 7 that the three methods of M1, M2 and M3 can make the flexible joint system effectively track the given trajectory, which indicates that the backstepping controller designed in this paper is effective. However, the steady-state errors of M2 and M3 have obvious oscillation convergence process, and the overshoots of M2 and M3 are larger than that of M1. In contrast, EFTPF can not only make the tracking error of flexible joint system converge in finite time, but also make the output have smaller overshoot and steady-state error. In Fig.7(d), the traditional PD control under the action of unknown disturbance will make the joint tracking error exceed the prescribed performance boundary, and the tracking effect is poor.

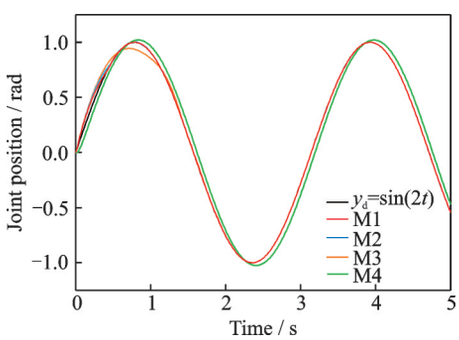

Fig.6 Position tracking

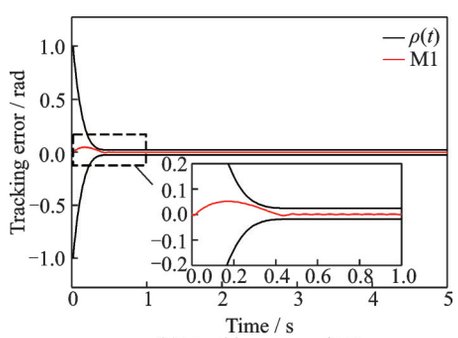

(a) Tracking error of M1

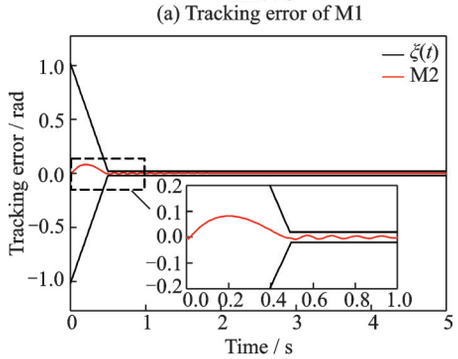

(b) Tracking error of M2

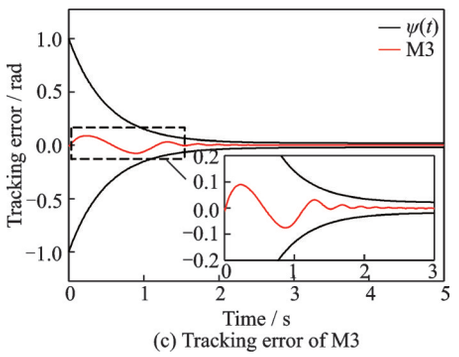

(c) Tracking error of M3

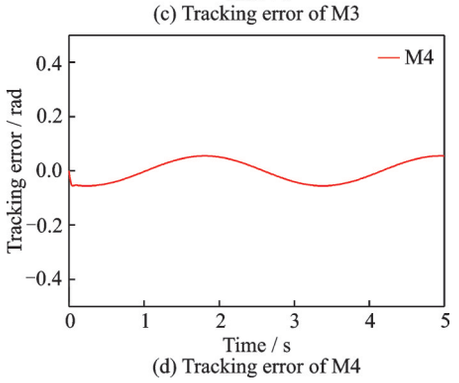

(d) Tracking error of M4

Fig.7 Tracking error

The joint control torque is shown in Fig. 8. It can be seen that the joint torque controlled by M1 and M2 has obvious oscillation convergence process at 0.5 s. This is reasonable, because M1 and M2 need to provide greater control torque when the time is close to T_1 to achieve the goal of error finite-time convergence. In contrast, the joint torque under M1 control has the fastest adjusting speed, while M3 has the longest adjusting time due to its lack of finite time convergence ability. The tracking results of tracking differentiator are shown in Fig.9. It can be seen that the tracking differentiator can not only effectively track the derivative signal of the virtual control law, but also reduce the signal noise. The estimation results of the unknown state observer are shown in Fig.10. Since the disturbance

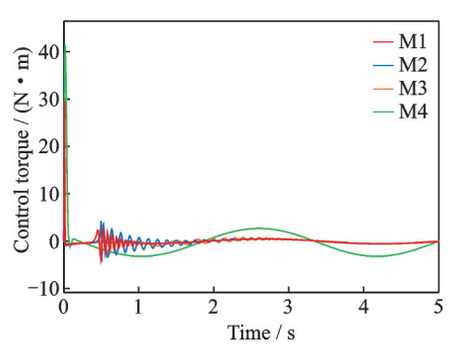

Fig.8 Joint control torque

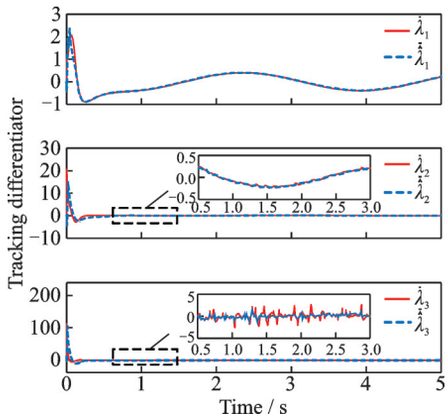

Fig.9 Output of tracking differentiator

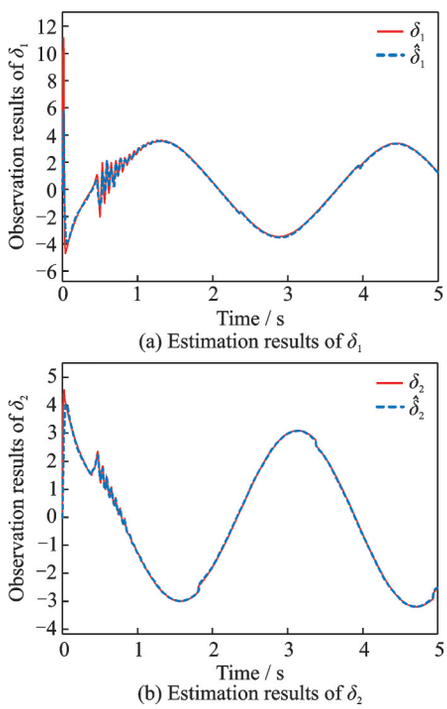

Fig.10 Estimation results of unknown dynamics

contains unmodeled dynamic terms related to joint position and velocity, the curves of δ_1 and δ_2 show obvious oscillation convergence process at 0.5 s. However, this does not affect the estimation results of the estimator, and the tracking of the lumped disturbance by the estimator is still accurate and effective.

When the given trajectory is a step signal with an amplitude of 0.5, the simulation results are shown in Figs.11—14. It can be seen from Figs.11 and 12 that compared with M2 and M3, the joint system under M1 control has smaller steady-state error and shorter adjustment time. This shows that even if the input signal is a discontinuous mutation signal, the proposed method can still guarantee the

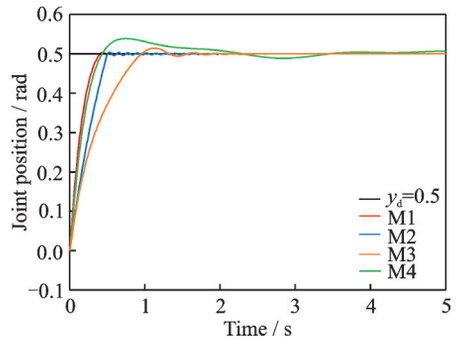

Fig.11 Position tracking

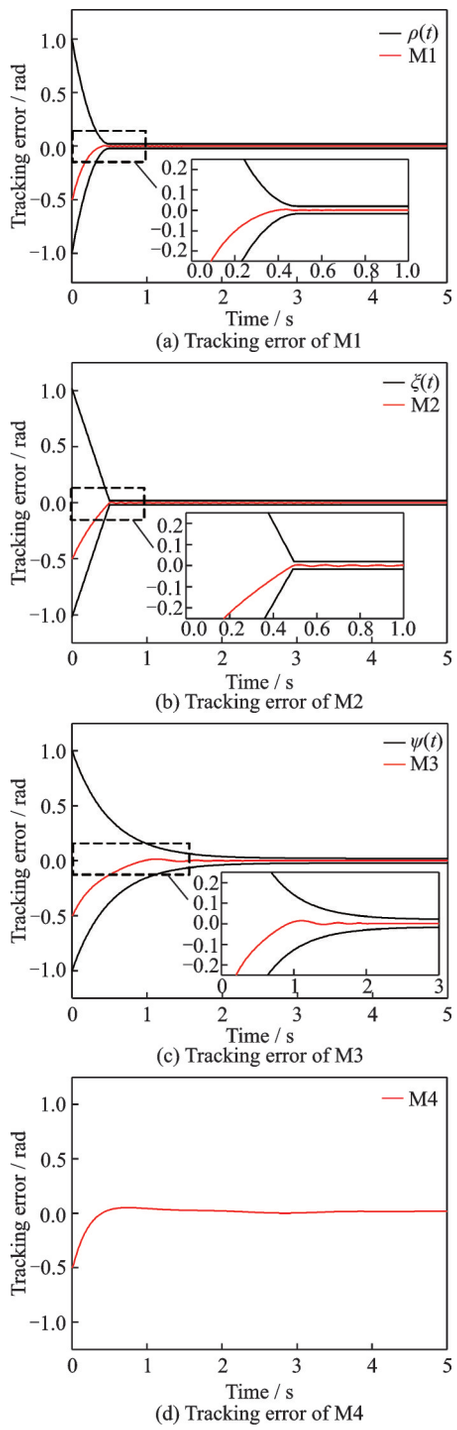

Fig.12 Tracking error

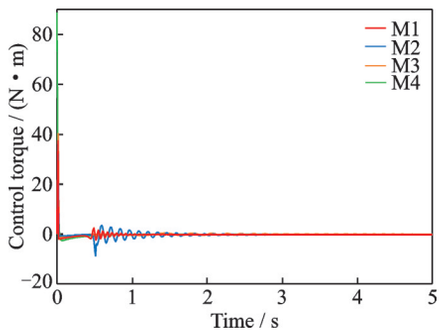

Fig.13 Control input

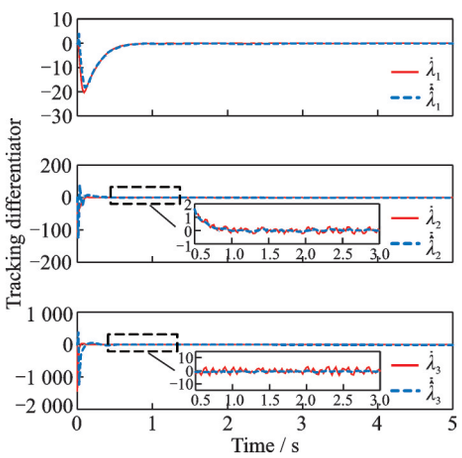

Fig.14 Output of tracking differentiator

joint has good transient and steady-state performance. The control input is shown in Fig.13. It can be seen that Fig.13 and Fig.8 have similar trends, but the difference is that the joint system under the action of step signal needs greater control torque in the process of starting, which is used to quickly reduce the tracking error. The tracking results of tracking differentiator are shown in Fig.14.

In summary, the proposed method M1 can ensure that the joint tracking error converges to a predetermined range in finite time, and improve the transient performance and tracking accuracy of the flexible joint system.

6 Conclusions

We propose a prescribed performance backstepping control method based on unknown state estimator and tracking differentiator for the flexible joint system with model uncertainty and external disturbance. The designed unknown state estimator can estimate the lumped disturbance only by the nominal value of the system model, and has less dependence on the model. The designed EFPTF has both exponential convergence trend and finite time convergence characteristics, and more conducive to limiting the system regulation time and overshoot. The backstepping controller is designed based on the EFTPF, and the uniform boundedness of all signals in the closed-loop system is proved. Furthermore, an improved tracking differentiator with both tracking rapidity and convergence stability is designed to estimate the derivative of the virtual control law, which solves the problem of controller differential explosion. Simulation results verify the effectiveness and advantages of the proposed method. The controller designed in this paper achieves the goal of converging the tracking error of the flexible joint to a predetermined range in a limited time, and improves the dynamic performance and control accuracy of the system.

References

[1] SONG Y X, WANG S X, LUO X Y, et al. Design and optimization of a 3D printed distal flexible joint for endoscopic surgery[J]. IEEE Transactions on Medical Robotics and Bionics, 2022, 4(1): 38-49.

[2] JIA S, SHAN J. Finite-time trajectory tracking control of space manipulator under actuator saturation[J]. IEEE Transactions on Industrial Electronics, 2020, 67(3): 2086-2096.

[3] CHEN Qiang, DING Xinke, NAN Yurong. Prescribed performance adaptive control of flexible-joint manipulators with output constraints[J]. Control and Decision, 2021,36(2): 387-394.(in Chinese)

[4] LIU X, ZHAO F. End-effector force estimation for flexible joint robots with global friction approximation usingneural networks[J]. IEEE Transactions on Industrial Informatics, 2019,15(3): 1730-1741.

[5] DAVIS H, BOOK W. Torque control of a redundantly actuated passive manipulator[C]//Proceedings of the 1997 American Control Conference. Albuquerque, NM,USA:IEEE,1997: 959-963.

[6] DONG F F, ZHAO X M, HAN J, et al. Optimal fuzzy adaptivecontrol for uncertain flexible joint manipulator based on D-operation[J]. IET Control Theory & Application. 2018, 12(9): 1286-1298.

[7] LE T L, ALBU S A. Robust adaptive tracking control based on state feedback controller with integrator terms for elastic joint robots with uncertain parameters[J]. IEEE Transactions on Control Systems Technology, 2018, 26(6): 2259-2267.

[8] ZHANG Y, LI Q, ZHANG W, et al. Weighted multiple neural network boundary control for a flexible ma-

nipulator with uncertain parameters[J]. IEEE Access, 2019, 7: 57633-57641.

[9] REN Y, ZHAO Z, ZHANG C, et al. Adaptive neural-network boundary control for a flexible manipulator with input constraints and model uncertainties[J]. IEEE Transactions on Cybernetics, 2021, 51(10): 4796-4807.

[10] XI R D, XIAO X, MA T N, et al. Adaptive sliding mode disturbance observer based robust control for robot manipulators towards assembly assistance[J]. IEEE Robotics and Automation Letters, 2022, 7(3): 6139-6146.

[11] XUE W, CHEN S, ZHAO C, et al. On integrating uncertainty estimator into pi control for a class of nonlinear uncertain systems[J]. IEEE Transactions on Automatic Control, 2021, 66(7): 3409-3416.

[12] XU Z, YANG S X, GADSDEN S A. Enhanced bio-inspired backstepping control for a mobile robot with unscented Kalman filter[J]. IEEE Access, 2020, 8: 125899-125908.

[13] NA J, CHEN A S, HERRMANN G, et al. Vehicle engine torque estimation via unknown input observer and adaptive parameter estimation[J]. IEEE Transactions on Vehicular Technology, 2018, 67(1): 409-422.

[14] BECHLIOULIS C P, ROVITHAKIS G A. Robust adaptive control of feedback linearizable MIMO nonlinear systems with prescribed performance[J]. IEEE Transactions on Automatic Control, 2008, 53(9): 2090-2099.

[15] NAI Y, YANG Q, WU Z. Prescribed performance adaptive neural compensation control for intermittent actuator faults by state and output feedback[J]. IEEE Transactions on Neural Networks and Learning Systems, 2021, 32(11): 4931-4945.

[16] LIU Y, LIU X, JING Y, et al. A novel finite-time adaptive fuzzy tracking control scheme for nonstrict feedback systems[J]. IEEE Transactions on Fuzzy Systems, 2019, 27(4): 646-658.

[17] SUN W, SU S F, XIA J, et al. Command filter-based adaptive prescribed performance tracking control for stochastic uncertain nonlinear systems[J]. IEEE Transactions on Systems, Man, and Cybernetics: Systems, 2021, 51(10): 6555-6563.

[18] SUI S, CHEN C L P, TONG S. A novel adaptive nn prescribed performance control for stochastic nonlinear systems[J]. IEEE Transactions on Neural Networks and Learning Systems, 2021, 32(7): 3196-3205.

[19] CUI G, YANG W, YU J, et al. Fixed-time prescribed performance adaptive trajectory tracking control for a QUAV[J]. IEEE Transactions on Circuits and Systems Ⅱ: Express Briefs, 2022, 69(2): 494-498.

[20] WEI Caosheng. Research on attitude prescribed performance control of spacecraft[D]. Xi'an: Northwestern Polytechnical University, 2019. (in Chinese)

[21] CHANG W, LI Y, TONG S. Adaptive fuzzy backstepping tracking control for flexible robotic manipulator[J]. IEEE/CAA Journal of Automatica Sinica, 2021,8(12): 1923-1930.

[22] LI Y, SHAO X, TONG S. Adaptive fuzzy prescribed performance control of nontriangular structure nonlinear systems[J]. IEEE Transactions on Fuzzy Systems, 2020, 28(10): 2416-2426.

[23] HAN Jingqiang, WANG Wei. Non-linear tracking-differentiator[J]. Journal of Systems Science & Mathematical Sciences,1994,14(2): 177-183.(in Chinese)

[24] CHEN Z, CHEN Q, HE X. Adaptive backstepping control design for uncertain rigid spacecraft with both input and output constraints[J]. IEEE Access, 2018, 6: 60776-60789.

[25] WANG Xinhua, CHEN Zengqiang, YUAN Zhuzhi. Nonlinear tracking-differentiator with high speed in whole course [J]. Control Theory & Application, 2003, 20(6): 875-878. (in Chinese)

[26] ZHAO Peng, YAO Minli, LU Changjie, et al. Design of nonlinear-linear tracking differentiator with high stability and high speed[J]. Journal of Xi'an Jiaotong University, 2011, 45(8): 43-48. (in Chinese)

[27] YANG Z, JI J, SUN X, et al. Active disturbance rejection control for bearingless induction motor based on hyperbolic tangent tracking differentiator[J]. IEEE Journal of Emerging and Selected Topics in Power Electronics, 2020, 8(3): 2623-2633.

[28] HE W, CHEN Y, YIN Z. Adaptive neural network control of an uncertain robot with full-state constraints[J]. IEEE Transactions on Cybernetics, 2017, 46(3): 620-629.

[29] LIU X, YANG C G, CHEN Z G. Neuro-adaptive observer based control of flexible joint robot[J]. Neurocomputing, 2018, 275: 73-82.

[30] NA J, JING B, HUANG Y, et al. Unknown system dynamics estimator for motion control of nonlinear robotic systems[J]. IEEE Transactions on Industrial Electronics, 2020, 67(5): 3850-3859.

[31] BHAT S P, BERNSTEIN D S. Finite-time stability of continuous autonomous systems[J]. SIAM Journal on Control and Optimization, 2000, 38(3): 751-766.

[32] DAI S L, HE S D, LIN H. Transverse function control with prescribed performance guarantees for underactuated marine surface vehicles[J]. International Journal of Robust and Nonlinear Control, 2019, 29(5): 1577-1596.

[33] CHEN Qiang, GU Xianyong, NAN Yurong, et al.

Funnel control of flexible-joint manipulators using an unknown system dynamics estimator[J]. Chinese High Technology Letters, 2022, 32(1): 66-76.(in Chinese)

[34] SHAO X L, WANG H L. Back-stepping robust trajectory linearization control for hypersonic reentry vehicle via novel tracking differentiator[J]. Journal of the Franklin Institute, 2016, 353(9): 1957-1984.

[35] GUO B Z, ZHAO Z L. On convergence of tracking differentiator[J]. International Journal of Control, 2011, 84(4): 693-701.

[36] HE S D, DONG C, DAI S L, et al. Cooperative deterministic learning and formation control for underactuated USVs with prescribed performance[J]. International Journal of Robust and Nonlinear Control, 2022, 32(5): 2902-2924.

[37] WANG Xinhua. Differentiator design and application-signal filtering and differentiation[M]. Beijing: Publishing House of Electronics Industry, 2010.(in Chinese)

Acknowledgements This work was supported by the National Natural Science Foundation of China (No.62076152), the National Natural Science Foundation of China (No. 62073200), the Natural Science Foundation of Shandong Province (No.ZR2020MF096), and funded by Beijing Advanced Innovation Center for Intelligent Robots and Systems.

Authors Mr. **SONG Chuanming** was born in 1995. He is a Ph.D. candidate in the School of Electrical and Electronic Engineering of Shandong University of Technology. His main research interests include humanoid robot control technology, special motor control technology, and power electronics and its control technology.

Prof. **DU Qinjun** received the Ph.D. degree in Bionic Technology from Beijing Institute of Technology, Beijing, China, in 2007. He is currently a professor and Ph.D. supervisor in Automation at the School of Electrical and Electronic Engineering, Shandong University of Technology. His current research interests include automation devices and control technology, humanoid robot control technology, intelligent production line control technology, and vehicle electrical and its control technology.

Author contributions Mr. **SONG Chuanming** designed this study, constructed a system model, proposed innovative methods, conducted analysis, and wrote manuscripts. Prof. **DU Qinjun** checked the correctness and rationality of the manuscript content and provided project support. Mr. **PANG Hao** helped to build the simulation model. Mr. **LI Cunhe** contributed to the analysis of simulation results. Prof. **JIAO Ticao** helped to analyze the stability of the system. All authors commented on the manuscript draft and approved the submission.

Competing interests The authors declare no competing interests.

(Production Editor: ZHANG Huangqun)

基于未知状态估计器和改进跟踪微分器的柔性关节预设性能反演控制

宋传明，杜钦君，庞　浩，李存贺，焦提操

（山东理工大学电气与电子工程学院，淄博 255049，中国）

摘要：为解决由模型不确定性和外部未知干扰导致的柔性关节系统控制偏差问题，提出一种基于未知状态估计器和跟踪微分器的预设性能反演控制方法。设计一种基于低通滤波器的未知状态估计器，该估计器仅依赖于模型的名义值即可估计集总扰动。构造了一种新的有限时间收敛预设性能函数，并基于该函数设计反演控制器，用于在保证闭环系统所有信号有界的情况下，使关节跟踪误差在约定时间内收敛到预定的任意小区域。为避免反演控制器的微分爆炸问题，设计基于改进Sigmoid函数的跟踪微分器来估计虚拟控制律的微分信号。仿真结果表明，在未建模动态和外部未知干扰的影响下，所提方法能够保证关节跟踪误差在有限时间内收敛到任意给定范围，有效提高了柔性关节的瞬态和稳态性能。

关键词：柔性关节；未知状态估计器；跟踪微分器；预设性能控制；反演控制